Hologram characterization in an optical memory experiment using photorefractive $LiNbO_3$

D. A. Woodbury, F. Davidson, T. A. Rabson, and F. K. Tittel

The design and performance characteristics of a computer interfaced optical memory system that utilizes holographic storage in photorefractive $LiNbO_3$ crystals are examined. An observed resolution limit of 145 μm (at 31 cm beyond the hologram) agrees closely with a 155-μm limit estimate based on spatial filtering and diffraction considerations. Angular and wavelength indexing are compared. A 3-D storage density limit of 10^{10} bits/cm^3 is estimated for angular indexing with the viewing angle optimized.

I. Introduction

Early considerations of volume holographic optical memories concluded that storage densities on the order of λ^{-3} for light of wavelength λ are theoretically possible.[1] For the visible range this implies a storage density of 10^{12} bits/cm^3, and the prospect of such high densities has motivated the study of volume holographic storage in photorefractive crystals such as $LiNbO_3$.[2–6] In these crystals the information is recorded as a spatially varying refractive index forming a phase hologram. Volume, or 3-D, storage is based on the superposition of 2-D holograms indexed by varying the Bragg condition for writing and readout.[1,7,8] Associated with this is the technique of thermal fixing to avoid erasure during superposition as well as to extend hologram lifetime.[10] Erasure during readout can be avoided by multiphoton writing, where the single-photon energy at readout is insufficient for photoexcitation.[11] Coherent erasure has been shown capable of selectively altering pages down to individual bits, leaving the other components virtually undisturbed.[12] Thus 3-D holographic storage in photorefractive crystals promises to be flexible technology for use in high density random access memories.

This paper describes the design and characterization of an experimental volume holographic optical memory system. In particular, the problems associated with the storage capacity of 2-D hologram pages and their superposition are discussed. The bit resolution was found to be limited by diffraction at the hologram image and spatial filtering at the hologram. Both angular and wavelength indexing were studied, and, with comparable separation criteria, angular indexing proved superior. Optimization of the viewing angle was found to be critical in maximizing the predicted 3-D storage density with angular indexing.

II. Experimental Procedures

The crystals used for this work were unannealed 0.05% iron-doped poled $LiNbO_3$ obtained from Crystal Technology. All hologram writing and reading were carried out with a cw argon-ion laser usually operated at 457 or 515 nm. The net writing intensity was 300 MW/cm^2 with a 30-sec exposure time that yielded a diffraction efficiency of about 50%. Angles of divergence and convergence were small, and lenses were not fully illuminated so that neither spherical aberration nor aperture diffraction patterns were a problem.

Figure 1(a) shows the configuration used in this work. A signal beam S was expanded and recollimated to a 1-cm FWHM beam that was passed through 2.5-cm diam lenses. The lens LS was used to focus the signal beam down to a hologram diameter h of roughly 1 mm in the crystal and to image the object at the detector. During readout the resulting hologram was self-focusing and required no additional lens. The lens LR focused the reference beam R to match the diameter of the S beam in the crystal. A shutter was used to block the signal beam during readout. As indicated by the dot–dashed lines, recorded diffracted waves from the object passed through an exit pupil determined by the hologram diameter. Holograms were recorded at an intersection near the R and S focal points, rather than at a common focal point, to avoid output distortions.

When this work was done all authors were with Rice University, Electrical Engineering Department, Houston, Texas 77001. D. A. Woodbury is now with General Dynamics Corporation, Fort Worth, Texas 76101, and F. Davidson is with Johns Hopkins University, Department of Electrical Engineering, Baltimore, Maryland 21218.

Received 26 July 1979.
0003-6935/80/050812-06$00.50/0.

The hologram output was detected using a P.A.R. 1205A/08 optical multichannel analyzer (OMA) operated in the 2-D mode. The OMA was interfaced with a PDP11/V03 minicomputer [as shown in Fig. 1(b)] so that the data from the OMA could be stored and processed conveniently. A single OMA scan consisted of 32 lines of 500 points each, and the OMA console was able to store on line of 500 points. The OMA detector was a silicon itensified target vidicon driven by the OMA console. The vidicon provided a preamplified analog pulse with a height that corresponded to the optical intensity detected at a given point. This pulse height was converted to binary coded decimal (BCD) by the OMA console for single-line operations. The BCD data were reconverted to analog by the console for real-time display on an XYZ monitor. The displays appeared as intensity modulated raster-scanned monitor traces. These displays were photographed and are referred to as OMA display data. A storage monitor was used here to make the roughly one picture per second appear to be a continuous display.

Data from the OMA vidicon detector were sent to the computer as follows: the OMA console converted the preamplified vidicon output pulse into a burst of 16-MHz clock pulses, whose burst length (total number of pulses) was proportional to the vidicon pulse height. The number of such pulses ranged from about 400 (vidicon dark current only) to a maximum of 950 (first-stage analog-to-digital conversion saturated). The useful linear range extended from about 400 to 740 such pulses. Each vidicon pulse corresponded to about two detected photons at the vidicon surface. These counts were gated to a pair of 12-bit binary counters. The contents of these counters were alternately stored in computer memory with the use of a direct memory access interface (DMA) at the rate of 22k words/sec. Each 32-line scan vidicon picture was initially stored as 16,000 words of 16 bits each in memory.

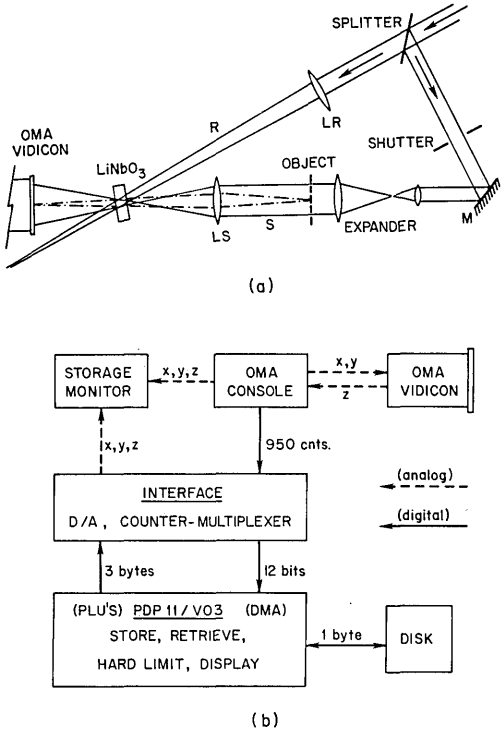

Fig. 1. Schematic of optical data acquisition system: (a) holographic storage arrangement with lens LS 13 cm from the object, focusing the signal beam S into the crystal 11 cm from LS and forming the image on the detector 31 cm from the crystal; (b) detection scheme using an OMA system.

The computer processed, displayed, and stored the data as follows. First, an operator-selected background count level was subtracted from each of the 16,000 picture elements. Adjacent picture elements were combined so that the number of elements per line was reduced from 500 to 250. This allowed each line to be displayed through the use of 8-bit digital-to-analog converters (ADCs). This caused a loss in horizontal resolution but gave an improved SNR for the vidicon signals, as will be discussed. The intensity at each of the resultant 8000 picture elements was divided by four so each could be represented as 8 bits (1 byte). The 8000 bytes were paired so they could be stored on a diskette as 4000 16-bit (2-byte) words. The entire 32-line pictures obtained in this way were displayed by the computer using thee 8-bit DACs to drive an XYZ monitor.

The vidicon is essentially a photon detector, and its output is statistical in nature, even when illuminated with constant intensity light. Since the holograms investigated were intended to store only binary information, they consisted of patterns of only light (illuminated) or dark (nonilluminated) regions. The optimal detection scheme[13] for recovery of these patterns using a photon detector consists of a comparison of the number of photocounts detected at any given point with a preselected threshold number of counts chosen to minimize the probability of error (deciding light was present when it was not and vice versa). If the number of such counts exceeded the threshold value, light was considered present. Each picture was compared against a preselected threshold and adjusted to full intensity or zero depending on the result of the comparison. This process is referred to as hard limiting in the subsequent discussion of our results.

The OMA vidicon detector area was spatially extended by translation of the vidicon so that a 2.5- × 2.5-cm^2 image area could be inspected. Usually data were taken over a total region consisting of about 200 lines of 1200 points each. In addition the intensified vidicon sensitivity allowed the use of filtering to cover a large range of optical intensities. Typically each vidicon position was investigated with one or two different filter factors. The resulting composite represented the complete image as if detected with a larger detector of greater dynamic range.

III. Results

Quantitative resolution measurements were based upon the single-line profiles obtained from the OMA as shown in Fig. 2. The objects used were sets of triple

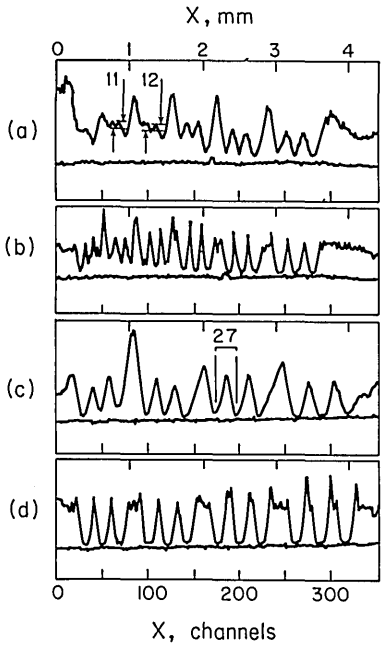

Fig. 2. Optical resolution characteristics depicted as single-line profiles from the OMA console: (a) hologram output for resolution bar chart with 11- and 12-channel separations satisfying Rayleigh criterion; (b) directly imaged object for Fig. 2(a); (c) hologram output for larger spacings showing 27-channel spacing similar to horizontal bit spacing in array study; (d) directly imaged object associated with Fig. 2(c). In all four cases the slowly curved line immediately under the data is the dark current background.

vertical bars from a resolution chart. The hologram outputs shown in Figs. 2(a) and (c) correspond to objects that appear directly imaged in Figs. 2(b) and (d), respectively. The Rayleigh criterion is satisfied for the two sets of bars shown in Fig. 2(a) with 11- and 12-channel spacings. The criterion requires a darkening to 81% of the maximum local intensity for the objects to be resolved, which is indicated by the arrows and horizontal marks. The 12.5-μm interchannel spacing on the vidicon together with the 11.5-channel average resolved separation imply a resolution limit of 145 μm for these outputs imaged at a distance of 31 cm from the crystal. As seen from Fig. 2(b), direct imaging of the object is well within these limits. Similar measurements indicated a 4-channel or 50-μm resolution limit for direct imaging. (The detector was 42 cm from the focusing lens *LS*.)

Figure 2(c) demonstrates the contrast ratio possible in the hologram output. Here only 5% of the maximum is detected in the images of the larger structures. However, the degree of smoothing or loss of detail remains in agreement with the resolution limit. The direct imaging of these structures is shown in Fig. 2(d). The bracketed 27-channel spacing in Fig. 2(c) roughly corresponds to the horizontal bit spacing used for a bit-array study described below.

It was necessary to optimize the positions of lenses *LS* and *LR* before holograms could be written reliably. The OMA display for the directly imaged object, a res-

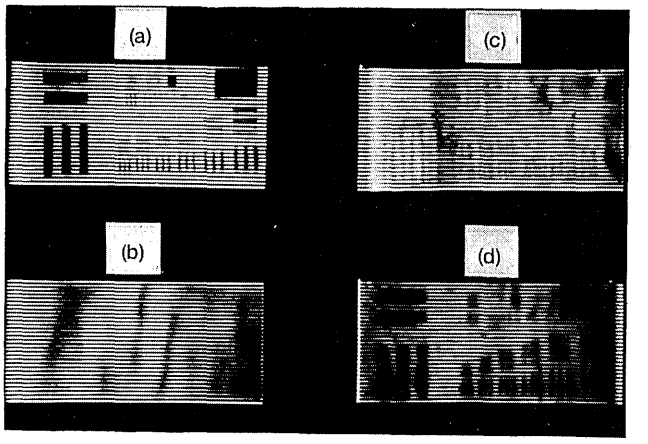

Fig. 3. Beam focusing: (a) directly imaged object with 50-μm resolution limit; (b) hologram output for both beams focused in crystal during writing; (c) output for *R* defocused but *S* still focused in crystal; (d) output when both *R* and *S* are defocused and matched at ~1-mm diameters.

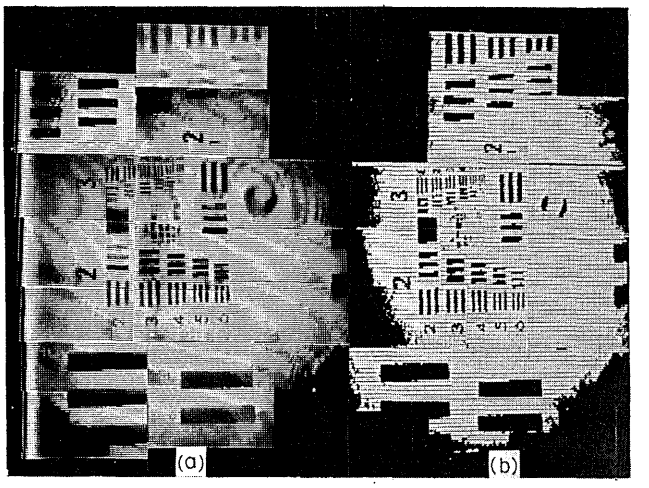

Fig. 4. Direct imaging of resolution chart on extended detector: (a) OMA display; (b) hard-limited data from computer.

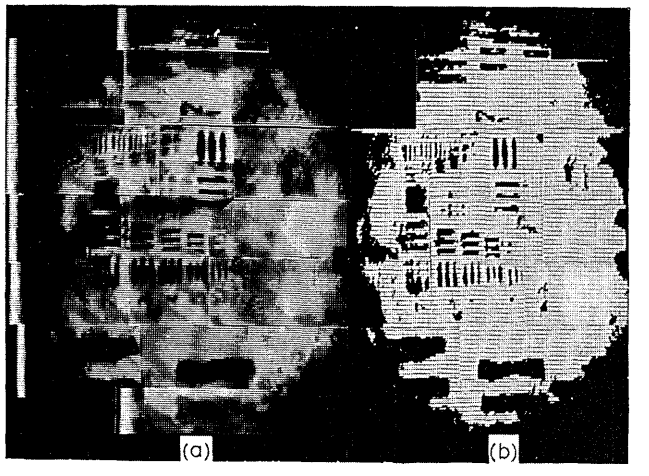

Fig. 5. Output of hologram of a resolution chart observed with extended detector: (a) OMA display; (b) hard-limited data.

olution chart, is shown in Fig. 3(a) resolved down to the 50-μm limit. The output from a hologram written with both beams focused in the crystal is shown in Fig. 3(b), where no structure was evident in the output. When R was defocused to a 1-mm spot in the crystal, a high degree of structure became evident, as shown in Fig. 3(c). However, the contrast appeared reversed and the image to be differentiated. Finally, when S was also defocused to match the 1-mm diameter of R in the crystal, the output, shown in Fig. 3(d), displayed the 145-μm limit and the correct contrast.

The absence of any detail in Fig. 3(b) can be attributed to the diffraction limit due to the hologram becoming of the order of the image size and its own spatial filter. The hologram size is crucial in determining both of these limits, and the focus of R defines this size in the crystal. The contrast reversal and image differentiation shown in Fig. 3(c) are interpreted as a loss of low spatial frequency components. These components are most likely suppressed by nonoptimized intensity-matching conditions for R during hologram writing. Here the sharply focused S wave has low frequency components at high intensity near the optic axis, while R is defocused and is more evenly distributed and less intense at that axis. Conversely, the high spatial frequency components in the S wave are distributed across the R wave and are more favorably intensity matched for holographic recording.

The results of extending the detector as described are evident in the OMA display composite of Fig. 4(a). This is a direct image of the resolution limit for direct imaging seems more than adequate. In Fig. 4(b) the same image data have been stored and processed using the PDP11 minicomputer. A series of 32-line 250-point/line zones were searched for thresholds that recovered the most detail. This was done to approximate a surface resembling the unmodulated beam profile and corresponding to a smooth variation of the filter factor and threshold across the image. In addition to enhancing greatly the appearance of the image, the hard-limiting procedure establishes that horizontal bars can be distinguished on alternate vidicon lines, i.e., at 200-μm vertical spacings.

The resolution chart was holographically recorded, and the extended OMA display of the output is shown in Fig. 5(a). Extensive convolution of both the R and S beams with modulation is apparent in the raw data. This output may be thought of as a blank hologram carrier beam that combines the R profile with the unmodulated S profile, which is in turn modulated by the object. Output image elements near the resolution limit are strongly disrupted by variations in the carrier, while those well within the limit are not seriously altered. The data of Fig. 5(a) were hard limited to produce Fig. 5(b). The threshold varied by a factor of 2, and the filtering was varied by a factor of 10, which permitted the intensity levels to be distinguished over a range of about 20–1. The smoothing of Figs. 5(a) and (b) corresponds to the 145-μm limit mentioned earlier. The horizontal bars appear separated at a spacing roughly 50% greater than that for the vertical bars.

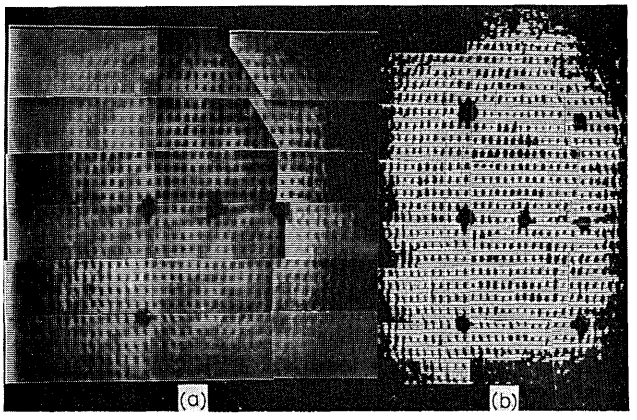

Fig. 6. Output of hologram written with bit array: (a) OMA display; (b) hard-limited data.

A bit array was stored holographically to characterize the variation of bit storage with location in the hologram output. The bit spacings were well within the 145-μm limit vertically and horizontally. As shown in Fig. 2(c), the horizontal spacing is about 27 channels or 340 μm at the detector, and the vertical spacing is 580 μm. The OMA display for the bit-array hologram output is shown in Fig. 6(a). The large structures are register marks. The hard limited data are shown in Fig. 6(b), which shows a continuous array of bits extending over the output. As before, an intensity range of about 20–1 was inspected. Hard limiting the data recovered 700 bits in this hologram. The 1.7–1 vertical-vs-horizontal bit spacings and the recovery of 34 rows of bits in other holograms [see Fig. 7(a)] imply 1k bits/hologram are recoverable.

Wavelength and angular indexing are physically similar,[7,8,14] and both methods were studied. Holograms were superimposed over one another at different wavelengths. Figures 7(a) and (b) shows the hard-limited outputs for a holograms written over one another at 457 and then 515 nm, respectively. Here 80–90% of the bits are recovered in the second hologram shown in Fig. 7(a), and the numerals remain quite recognizable. The first hologram was written with twice the exposure as the second hologram to compensate for erasure. The output of the first hologram written at 457 nm is shown in Fig. 7(b) after superposition. Here only 50% of the bits are recovered, and fringes are apparent in the output that suggest interference with the other hologram output.

The 600-Å separation used in wavelength indexing was used to infer a 0.7° separation for angular indexing, as discussed below. Holograms were angularly indexed at this separation, and the hard-limited outputs for two of these are shown in Figs. 7(c) and (d). The results are markedly better than for the wavelength-indexed holograms of Figs. 7(a) and (b). Eighty percent of the bits are recovered in both the angularly indexed holograms, and no fringes are visible. Angular indexing is the method assumed in 3-D storage-density estimates discussed below.

IV. Discussion

Three-dimensional storage density depends on 2-D capacity of a hologram page and the capacity of a thick medium to hold superimposed hologram pages.[1,7,8] The 2-D storage density for circular image-filling arrays stored as circular holograms in a square lattice is given as

$$\mathcal{D} = \frac{\pi}{4}\left(\frac{\epsilon D}{hd}\right)^2. \tag{1}$$

Here h is the hologram diameter, ϵ is a filling factor allowing for spacings greater than h, d is the resolution limit or minimum bit spacing, and D is the image diameter. The resolution results indicate $d = 145\ \mu$m at 31 cm for $h = 1$ mm. Thus, $\mathcal{D} = 210$k bits/cm^2 is the resolution-limited 2-D storage density for $D = 1.5$ cm and assuming $\epsilon = 1/2$ in this arrangement.

The resolution limit may be attributed to diffraction effects associated with the hologram diameter. The appropriate form to use concerning a hologram output is the Rayleigh resolution limit. This requires the first minimum of one output element diffraction pattern to fall on the maximum of the next. The limit then becomes

$$d = \lambda z/h \tag{2}$$

with z being the hologram-to-image distance (31 cm). Equation (2) may also be obtained based on spatial filter arguments, where d is taken as the fringe spacing for two sources at opposite boundaries of the hologram.[15] Specifically, for $d \ll z$ the interfering wave fronts are nearly planar over the region of interest so that $d = \lambda/2 \sin\theta$ for a half angle θ. Then for $h \ll z$ the small-angle approximation holds so that $2 \sin\theta \cong 2\theta \cong h/z$ in agreement with Eq. (2). Another argument concerns the recording ability of the hologram, which depends on the beat frequency between independent sinusoidal components. These components yield critically resolved image elements at far field. The beat frequency is limited by $1/h$, and if the components have grating spacings x and x', they can only be distinguished if they are recorded over the distance $(1/x - 1/x')^{-1} \leq h$. This last condition yields $d = \lambda z/h \cos\theta$, which is within a few percent of Eq. (2) for half angles of $\theta \leq 15°$.

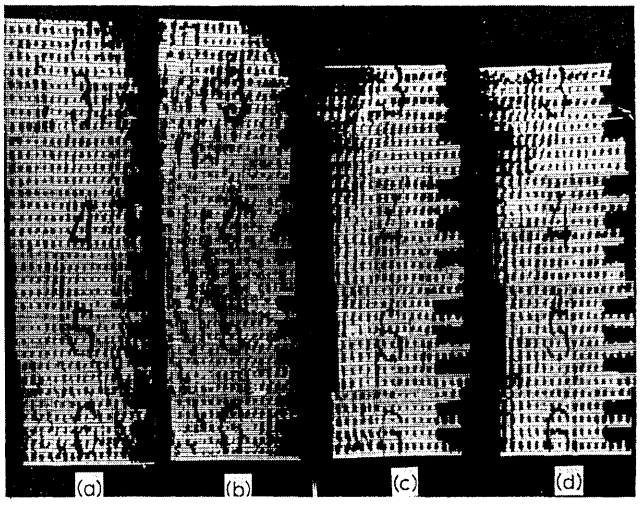

Fig. 7. Indexing: (a) hologram written at 515 nm; (b) at 457 nm; (c), (d) angularly indexed holograms separated by 0.7°.

As shown, diffraction and spatial filtering considerations give equivalent estimates of the resolution limit for hologram recording and readout. Equation (2) indicates a limit of 155 μm for $z = 31$ cm and $h = 1$ mm, which is in close agreement with the observed limit of 145 μm. Using $d = 155\ \mu$m in Eq. (1) lowers the estimated 2-D density to $\mathcal{D} = 180$k bits/cm^2. Consequently, the average values of $d \cong 150\ \mu$m and $\mathcal{D} \cong 200$k bits/cm^2 seem reasonable.

Equations (1) and (2) may be combined to put the estimate in terms of a viewing angle $F = D/z$, where the result takes the form

$$\mathcal{D} = \frac{\pi}{4}\left(\frac{\epsilon E}{\lambda}\right)^2 \tag{3}$$

and is independent of h. This general form may be multiplied by $2/\pi$ to consider square arrays. Other estimates[6,16] of $\mathcal{D}$ are similar in form with the diffraction limit chosen differently. Aperture ratio magnification and other parameters may be optimized,[16] but Eq. (3) specifies the upper limit on 2-D storage density.

Holograms were also recorded using bit arrays with bit spacings well within the resolution limit discussed. Approximately $N = 10^3$ bits/hologram were recovered. The corresponding storage density is given by $\mathcal{D} = N(\epsilon/h)^2$, which implies 25k bits/cm^2. There is an asymmetry of $d_y = 1.7 d_x$, where d_y and d_x are the vertical and horizontal spacings, respectively. This asymmetry and the use of a horizontal bit spacing that is twice the resolution limit imply a storage density of $(1.7 \times 2 \times 2)^{-1} = 0.15$ times the resolution-limited estimate. Thus, 0.15×200k bits/cm^2 = 30k bits/cm^2 is the expected density in good agreement with the 25k-bit/cm^2 storage density achieved.

Wavelength indexing results shown in Figs. 7(a) and (b) indicate that greater than 600 Å is needed to avoid interference of the outputs. The Bragg condition $\lambda = 2\Lambda \sin\theta$ may be differentiated to yield

$$\delta\theta = \frac{\delta\lambda}{2\Lambda \cos\theta} = \frac{\delta\lambda}{\lambda}\tan\theta. \tag{4}$$

Then Eq. (4) may be used to convert the 600-Å wavelength separation to a corresponding angular separation of 0.7°. This angular separation is more than adequate as shown in Figs. 7(c) and (d) compared with the wavelength indexing result shown in Figs. 7(a) and (b). Considering that the two choices of separation ought to be roughly equivalent, this is evidence that angular indexing is the better method of superposition.

The total useful angle Φ and the crystal or beam rotation angle $\Phi - F$ determine the number of superpositions M as

$$M = (\Phi - F)/\delta\theta. \tag{5}$$

For a typical value of $\Phi = 60°$, Eq. (5) indicates that

eighty holograms could be superimposed (with fixing) based on the $F = 2.8°$ view angle used here. The resolution-limited 2-D density of $\mathcal{D} = 200$k bits/cm^2 and an effective thickness[14] of ~0.5 mm in this material imply a 3-D density of $\Delta = M\mathcal{D}/t = 320$M bits/cm^3. The stored bit-array results imply a Δ about ten times smaller.

A theoretical estimate of the 3-D storage density can be obtained from Eqs. (3) and (5) as

$$\Delta = \frac{MD}{t} = \frac{\pi}{4t}\left(\frac{\Phi - F}{\delta\theta}\right)\left(\frac{\epsilon F}{\lambda}\right)^2. \tag{6}$$

This expression can be maximized as a function of F, and $F = (2/3)\Phi$ is shown to be the optimum choice of view angle. Using this view angle, the resolution-limited 2-D density is 4×10^7 bits/cm^2, and the 3-D density is 2×10^{10} bits/cm^3. As before, the bit-array results are about 1/10 of this. Severe distortions and beam matching problems inhibit the use of total angles of much more than $\Phi = 60°$, but in principle another factor of 10 could be gained if such problems were overcome.

The holograms were detected with the use of a silicon intensified target (SIT) vidicon of a sensitivity such that one OMA count corresponded to about two detected photons. Each point in the reconstructured holograms produced by the computer had a SNR (a ratio of the mean number of photons to one standard deviation of the mean) of at most $(700)^{1/2}$ or about 27:1. This number is obtained by subtraction of the constant dark current (400) from the maximum number of counts on the linear range of the OMA (750) and combining two such picture elements into one for display purposes. The SNR characterizes only the detection of light at a single point in the reconstructed hologram by a detection that functions through photon absorption. It does not include effects in the output hologram due to imperfections in the storage medium or associated optics. The quality of the reconstructed holograms can be improved substantially in terms of closer correspondence to the original 2-D pattern it represents through the use of phase-coded or phase-diffused reference beams.[17,18]

Considerably better SNR and lower background or dark current could be obtained with the use of a secondary electron conduction (SEC) vidicon. Although SEC vidicons have lower luminous sensitivities than SIT vidicons, they have much larger linear dynamic ranges, much lower leakage or dark currents, and much longer image storage times. The resultant SNR is much larger since each OMA corresponds to a much larger number of detected photons at the vidicon surface. The only restriction on the use of SEC vidicons as detectors is that the holograms must be reconstructed with a strong enough laser beam that the bright (or illuminated) regions are intense enough to be well above the minimum level detectable by the SEC vidicon and yet not so intense as to erase the hologram in the storage crystal.

Better performance in terms of recovery of the stored binary information from the hologram could be obtained through the use of storage formats more complicated than simple light (digital one) or dark (digital zero) regions of the hologram. This format is the 2-D equivalent of temporal ON–OFF binary signaling. It is well known that for direct detection optical communication systems, binary pulse position modulation formats (BPPM) give much better performance in terms of bit error rates than ON–OFF signaling given equal total amounts of received light energy. The optimal detector for such formats involves comparisons of received signals not against fixed thresholds but with other received signals. In a BPPM system the detector records total energy received in each half of a signal interval and chooses the binary signal (one or zero) that corresponds to the received sequence (e.g., more energy in the first half of the interval than the second). The 2-D equivalent of this format would be a checkerboard array of a light region followed by a dark and vice versa. The optimal detector for this pattern would simply compare vidicon signals from two adjacent regions and determine which signal is larger. This type of storage format would completely circumvent problems that arise in the fixed threshold ON-OFF format due to nonconstant dark currents over the entire vidicon surface and due to intensity variations across the reading and writing laser beams. The only disadvantage is that precise alignment of the holograms with the vidicon is required.

The experimental results show that hologram output is limited by diffraction due to the hologram diameter and spatial filtering. The two interpretations are essentially equivalent yielding the familiar form of Eq. (2). The 2-D storage density limit is independent of the hologram diameter and around 200k bits/cm^2 for the view angle used. Angular and wavelength indexing were studied with angular indexing proving to be the more reliable of the two. A 3-D storage density was estimated to be 3×10^8 bits/cm^3 for a useful angle of 60° and 10^{10} bits/cm^3 when the viewing angle is optimized. These results offer strong endorsement for the use of holographic storage in photorefractive crystals for optical random access memories and read-write memories.

This work was supported by the National Science Foundation and the U.S. Army Ballistic Missile Defense Advanced Technology Center.

References

1. P. J. van Heerden, Appl. Opt. 2, 393 (1963).
2. L. D'Auria, J. P. Huignard, C. Slezak, and E. Spitz, Appl. Opt. 13, 808 (1974).
3. H. Kurz, Opt. Acta 24, 463 (1977).
4. W. J. Burk, D. L. Staebler, W. Phillips, and G. A. Alphonse, Opt. Eng. 17, 308 (1978).
5. A. M. Glass, Opt. Eng. 17, 470 (1978).
6. J. P. Huignard, in *Proceedings, Lasers 75 Optoelectronic Conference*
7. L. D'Auria, J. P. Huignard, and E. Spitz, IEEE Trans. Magn. MG-9, 83 (1973).
8. H. Kogelnik, Bell Syst. Tech. J. 48, 4909 (1969).
9. W. J. Burke and Ping Sheng, J. Appl. Phys. 48, 681 (1977).
10. D. L. Staebler, W. J. Burke, W. Phillips, and J. J. Amodei, Appl. Phys. Lett. 26, 182 (1975).
11. D. von der Linde, A. M. Glass, and K. F. Rodgers, J. Appl. Phys. 47, 217 (1976).
12. J. P. Huignard, J. P. Herriau, and F. Micheron, Ferroelectrics 11, 393 (1976).
13. R. M. Gagliardi and S. Karp, *Optical Communications* (Wiley, New York, 1976), Chap. 5.
14. D. A. Woodbury, T. A. Rabson, and F. K. Tittel, Appl. Opt. 18, 255 (1979).
15. M. V. Klein, *Optics* (Wiley, New York, 1970), p. 443.
16. A. Vander Lugt, Appl. Opt. 12, 1675 (1973).
17. T. F. Krile, R. J. Marks II, J. F. Walkup, and M. O. Hagler, Appl. Opt. 16, 3131 (1977).
18. J. T. LaMacchia and D. L. White, Appl. Opt. 7, 91 (1968).